HiSST: International Conference on
High-Speed Vehicle Science Technology
26–29 November 2018, Moscow, Russia

Detailed mathematical and numerical investigations of shock wave-boundary layer interaction in hypersonic flows

Sterian Dănăilă[1], Alina Bogoi[1], Dragoș Isvoranu[1] and Constantin Leventiu[1]

Abstract

Present paper is a two-step investigation of some benchmark problems in the field of supersonic/hypersonic phenomena. The first step is concerned on the assessment of three Weighted Essentially Non-Oscillatory (WENO) type numerical schemes for shock tube problems applied for simple cases, like scalar conservation law. The idea is to objectively present the performances of these numerical schemes covering a wider range of Riemann problems and not only on some specific favourable cases as it is customary done in specialized literature. All the schemes identify accurate the position of the shock and converge to the proper weak solution for non-linear flux and different initial conditions. Next, the paper refers to the unsteady laminar or turbulent shock wave/boundary layer interactions over compression ramps with a sharp leading edge. The in-house code that has been developed (SUPERHYP) solves the time-dependent conservation law form of the RANS/LES equations. This code is Fortran parallel code with a graphical interface to survey the solution during run. The spatial discretization involves a finite-volume approach. Upwind-biasing is used for the convective and pressure terms, while central differencing is used for the shear stress and heat transfer terms. Time advancement strategy allows solving steady or unsteady flows. Grids must be supplied, but a mesh generator for simple geometries is included in the package

Keywords: *shock wave, boundary layer, WENO, Superhyp*

1. Introduction

It is a well-known fact that numerical simulations, especially DNS and LES, require high resolution discretization techniques in both space and time domains. One major challenge in applying these techniques is the constant pursuit for reducing the numerical dispersion and diffusion bellow the dispersion and diffusion inherent to the physical phenomenon modelled by the numerical scheme. On the other hand, the increased order of accuracy necessitates enlarging the numerical stencil which leads to a larger computational effort. Another drawback of the high order schemes is associated with the unphysical oscillations generated near discontinuities (shock waves or shear flows). Hence, a thorough analysis of the accuracy of various numerical schemes is required to pinpoint the behaviour of these techniques in the presence of flow discontinuities.
In the first part of the present paper, we analyse in detail a series of test cases for which the exact analytical solution has been produced and could serve as a better ground for accuracy prediction of the tested high order numerical schemes. In the frame of spatial discretization, we are interested in two essential steps in solution procedure: reconstruct the physical fields to find the values at the left- and right-sides of cell boundaries and evaluate the numerical fluxes at cell boundaries required in the finite volume method (FVM) formulation to update the cell-integrated values for next time step. For the first step, four different reconstruction schemes are analysed: the original Weighted Essentially Non-Oscillatory (WENO) scheme [1], Mapped WENO (WENO-M) [2], Compact Reconstruction WENO (CRWENO) schemes [3] and WENO-Z scheme [4].The main interest is limited to present comparisons of numerical tests. Interested readers are referred to cited articles for theoretical background.The evaluation of the numerical fluxes at cell boundaries is needed to update the cell-integrated values for next time step and to solve the exact Riemann problem at the cell's boundary in the FVM formulation. In this paper, for the second step we use the following typical numerical fluxes: the Roe

[1] *Depart. of Aerospace Sciences, University Politehnica of Bucharest, 1-7 Gheorghe Polizu Str., 011061-Bucharest, ROMANIA, sterian.danaila@upb.ro, bogoi_alina@yahoo.com,ddisvoranu@gmail.com, cleventiu@yahoo.com*

flux [5], the HLL (Harten–Lax-van Leer) flux [6], the Lax–Friedrichs flux [1], the HLLL (Harten–Lax-van Leer -Linde) flux[7] and the AUSM flux[8]. Numerical schemes based on linear approximation often produce spurious oscillations and overshoots near discontinuities especially when the solution has non-smooth behaviour (such as expansions, shocks or contact discontinuities).
The second part of the paper refers to numerical resolution of shock wave/boundary layer interaction problem in supersonic/hypersonic flows. The physical features of a shock wave/boundary layer interaction in the hypersonic regime are extensively presented in the works of Chapman et al. [9], Anderson[10], Green [11], Holden [12] and Marini [13]. Experimental studies of both laminar and turbulent shock wave/boundary-layer interactions from supersonic through hypersonic regime were published by Holden [12], Settles et al.[13] and Kuntz et al [15]. The palette of cases covers a wide range of Mach and Reynolds numbers. Numerical results are compared with available experimental results. It is shown that the accuracy of the numerical data depends strongly on ramp angle and Reynolds number.

2. Assessment of some high-order schemes

2.1. Problem formulation

Many fluid dynamics applications ranging from turbulence to acoustics include propagation of nonlinear waves with a continuous or discontinuous distribution of the physical variables. Rarefaction fans, shocks or contact discontinuities are elementary waves that make upthe solution of Riemann problem for hyperbolic equations, like Euler equations [5, 6]. The aim of the present work is a new comparison of the behaviour of the 5th-order WENO-type numerical methods: the classical WENO-JS [16, 17, 18], the mapped WENO [2], the compact reconstruction WENO [3] and the WENO-Z [4, 7].
Let us consider the initial value problem of the one-dimensional vector conservative equation $\forall t \geq 0,\ x \in \mathbb{R}$:

$$\frac{\partial \mathbf{U}}{\partial t} + \frac{\partial \mathbf{F}(\mathbf{U})}{\partial x} = \mathbf{0}, \quad \mathbf{U}(x,0) = \mathbf{U}_0(x), \tag{1}$$

where $\mathbf{U}(x,t)$ and $\mathbf{F}(\mathbf{U}(x,t))$ are the conservative variables and respectively the conservative flux vector defined by:

$$\mathbf{U} = \left(\rho, \rho u, \rho E\right)^t, \quad \mathbf{F} = \left(\rho u, \rho u^2 + p, u(\rho E + p)\right)^t \tag{2}$$

and $\mathbf{U}_0(x)$ is the initial condition. Density ρ, velocity u, pressure p are related to the total energy E by the calorically perfect ideal gas equation of state

$$p = (k-1)\rho\left(E - u^2/2\right) \tag{3}$$

with k the ratio of specific heats being constant and equal to1.4.
The numerical solution is obtained by discretizing the equation in space and time.
Discretizing the spatial derivative for each corresponding point $x_j = j\Delta x,\ j = \overline{0,N}$, the following conservative finite difference scheme results:

$$\frac{\mathrm{d}\mathbf{U}_j}{\mathrm{d}t} + \frac{\mathbf{F}^*_{j+1/2} - \mathbf{F}^*_{j-1/2}}{\Delta x} = 0. \tag{4}$$

Thus, we get a system of ordinary differential equations for $\mathbf{U}_j(t) = \mathbf{U}(x_j, t)$. The term $\mathbf{F}_{j+1/2}$ is the numerical flux at cell boundaries computed by a Riemann solver $\mathbf{F}^*_{j+1/2} = \mathbf{F}^{\text{Riemann}}(\mathbf{U}^L_{j+1/2}, \mathbf{U}^R_{j+1/2})$.
The solution of the conservative finite difference formulation of Eq. (1) written in the semi-discrete form, Eq. (4), consists of two steps: spatial discretization and time marching, respectively.

2.2. Spatial and temporal discretization

As mentioned before four different reconstruction schemes are analyzed: the original Weighted Essentially Non-Oscillatory (WENO) scheme, Mapped WENO (WENO-M), Compact Reconstruction WENO (CRWENO) schemes proposed by Ghosh and Baeder [3] and WENO-Z scheme. To estimate the numerical flux at the cell boundary we use the following typical numerical fluxes: the Roe flux, the

HLL (Harten–Lax-van Leer) flux, the Lax–Friedrichs flux, the HLLL (Harten–Lax-van Leer -Linde) flux and the AUSM flux.
The numerical solution of the scalar conservation law is semi-discretized in the spatial domain using a discrete set of points. After the spatial partial derivatives have been replaced with appropriate finite differences in x_j, we get the following system of ODE's:

$$\frac{\mathrm{d}\mathbf{U}}{\mathrm{d}t} = L(\mathbf{U}(t)),\ L(\mathbf{U}_j) = -\frac{\mathbf{F}\left(\mathbf{U}(x_{j+1/2},t)\right) - \mathbf{F}\left(\mathbf{U}(x_{j-1/2},t)\right)}{\Delta x}, \tag{5}$$

where the discrete operator L is used to solve each ODE in time. Here, we associate the time dependent vector $\mathbf{U}(t)$ with $\mathbf{U}_j(t) = \mathbf{U}(x_j,t),\ j = \overline{0,N}$.
The time discretization will be implemented using a third-order TVD Runge–Kutta (TVDRK3) developed by Shuand Osher [10].

$$\mathbf{U}^{(1)} = \mathbf{U}^n + \Delta t L(\mathbf{U}^n) \tag{6}$$

$$\mathbf{U}^{(2)} = 0.75\mathbf{U}^n + 0.25\mathbf{U}^{(1)} + \Delta t L(\mathbf{U}^{(1)}) \tag{7}$$

$$\mathbf{U}^{n+1} = \mathbf{U}^n / 3 + 2\mathbf{U}^{(2)} / 3 + 2\Delta t L(\mathbf{U}^{(2)}) / 3 \tag{8}$$

2.3. Numerical tests

In this section, we present the numerical results of some typical benchmark shock-tube tests for 1D Euler equation with different Riemann initial conditions. The main purpose is to capture the salient features and to present objectively the capacity of each WENO method to solve the shock tube problem with different initial conditions. These benchmark tests are most relevant in order to check and to identify accurate the position of the shock, contact and rarefaction waves in each situation.
The shock tube problem considers a long, thin, cylindrical tube of gas separated by a thin membrane. The gas is assumed to be at rest on both sides of the membrane, but it has different constant pressures and densities on each side. At time $t = 0$, the membrane is ruptured and the problem is to determine the ensuing motion of the gas which generates a nearly *centred* wave system that typically consists of a rarefaction/shock wave, a contact discontinuity and a shock/rarefaction wave. The middle wave is always a contact discontinuity while the left and right (non-linear) waves are either shock or rarefaction waves. Therefore, according to the type of nonlinear waves there can be four possible wave patterns [6]. This physical problem is reasonably well approximated by solving the shock-tube problem for the Euler equations. This problem was first studied by Riemann, and known as the Riemann problem. The solution to this problem consists of a shock wave moving into the low-pressure region, a rarefaction wave that expands into the high-pressure region, and a contact discontinuity which represents the interface. The computational domain is taken as $[0,\ 1]$. In most of the numerical tests at $x = 0$ and at $x = 1$ zero gradient boundary conditions are considered. Any other situations will be specifically mentioned.

a. Sod's shock tube problem (expansion-contact-shock)
The initial condition for the Sod problem [6] is

$$(\rho,\ u, p) = \begin{cases} (1,0,1), & 0 \le x < 0.5 \\ (0.125,0,0.1), & 0.5 \le x \le 1 \end{cases} \tag{9}$$

and the final time is $t = 0.15$. The grid resolution is 400 cells and the time stepping condition is CFL = 0.3. Fig. 1 illustrates well resolved shock and contact solutions.
Predictions given by the WENO-type schemes are indistinguishable at the scale shown. Nevertheless, the numerical solution displays a gradual departure from the analytical solution in the regions with sharp slopes.

b. Lax's shock tube problem (expansion-contact-shock)
The initial condition for the Lax problem [6] is

$$(\rho,\ u, p) = \begin{cases} (0.445,0.698,3.528), & 0 \le x < 0.5 \\ (0.5,0,0.571), & 0.5 \le x \le 1 \end{cases} \tag{10}$$

and the final time is $t = 0.12$. Fig.2 shows no spurious oscillations at any shock or contact discontinuities.

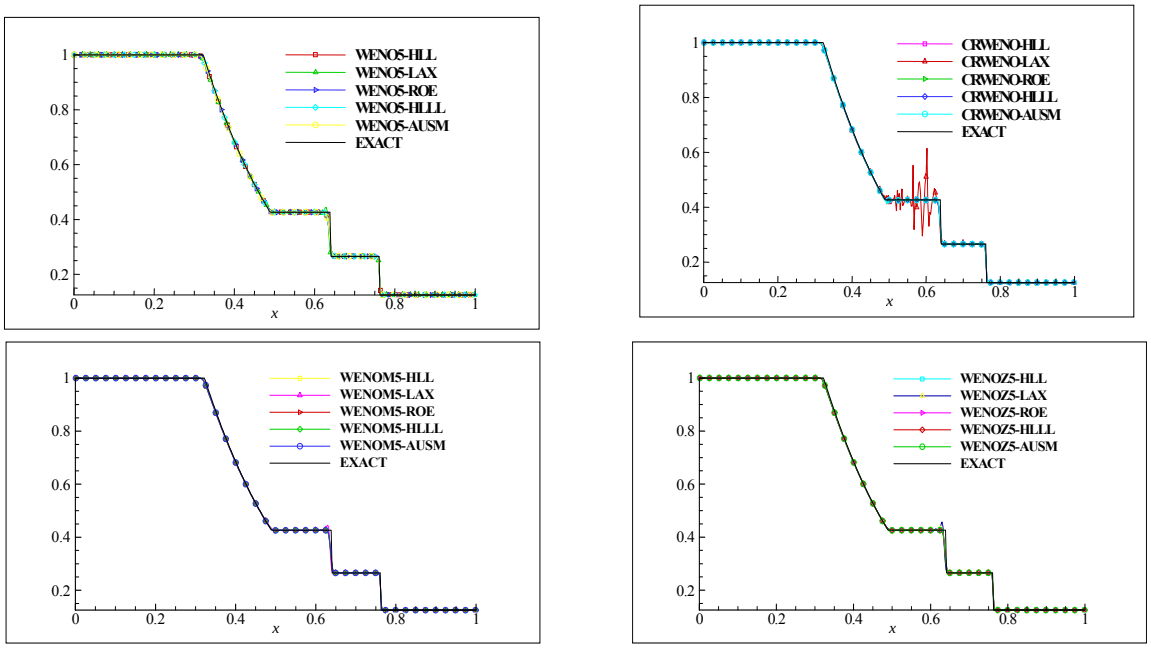

Fig. 1. Numerical results for the density for Sod's shock tube problem at t = 0.15.

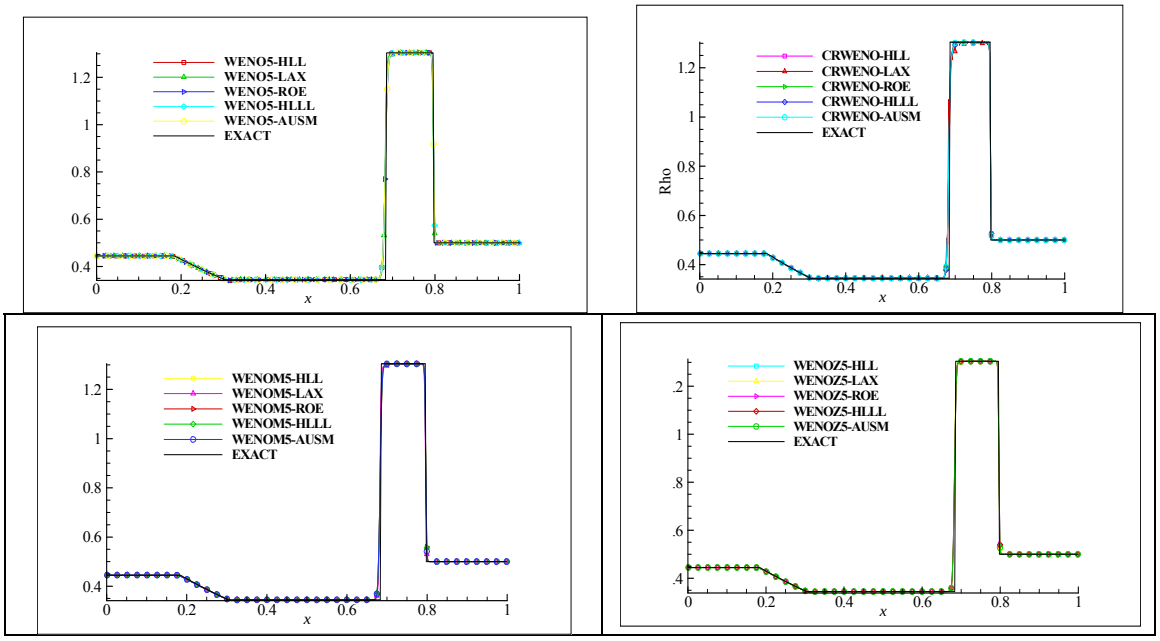

Fig. 2. Numerical results for the density for the Lax's shock tube problem at t = 0.12.

c. Strong shock tube problem (expansion-contact-shock)

The initial condition for the strong shock tube problem [8] is

$$(\rho, u, p) = \begin{cases} (1, 0, 10^{10}), & 0 \le x < 0.5 \\ (0.125, 0, 0.1), & 0.5 \le x \le 1 \end{cases} \tag{10}$$

and the final time is $t = 2.5 \cdot 10^{-6}$. This initial condition creates a supersonic shock associated with extreme jumps in velocity and pressure, see Fig.3a. It is well known that purely non-conservative schemes fail to compute strong shocks due to their intrinsic inability to calculate the correct shock speeds Fig.3b shows there are density overshoots in results but correct shock calculation. We have also remarked that AUSM scheme does not converge in most of the cases. The only case where it works (N.B. but not very accurate), is with CRWENO method. Instead, Lax flux gives high oscillations in the vicinity of the contact wave.

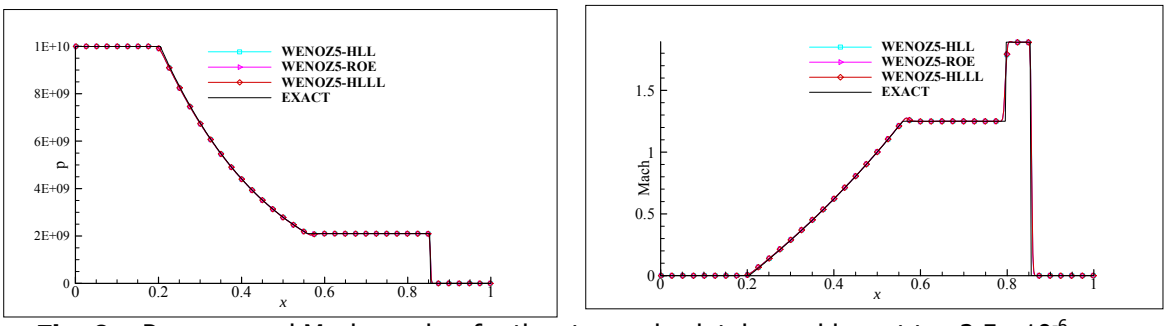

Fig. 3a. Pressure and Mach number for the strong shock tube problem at t = 2.5 · 10^{-6}.

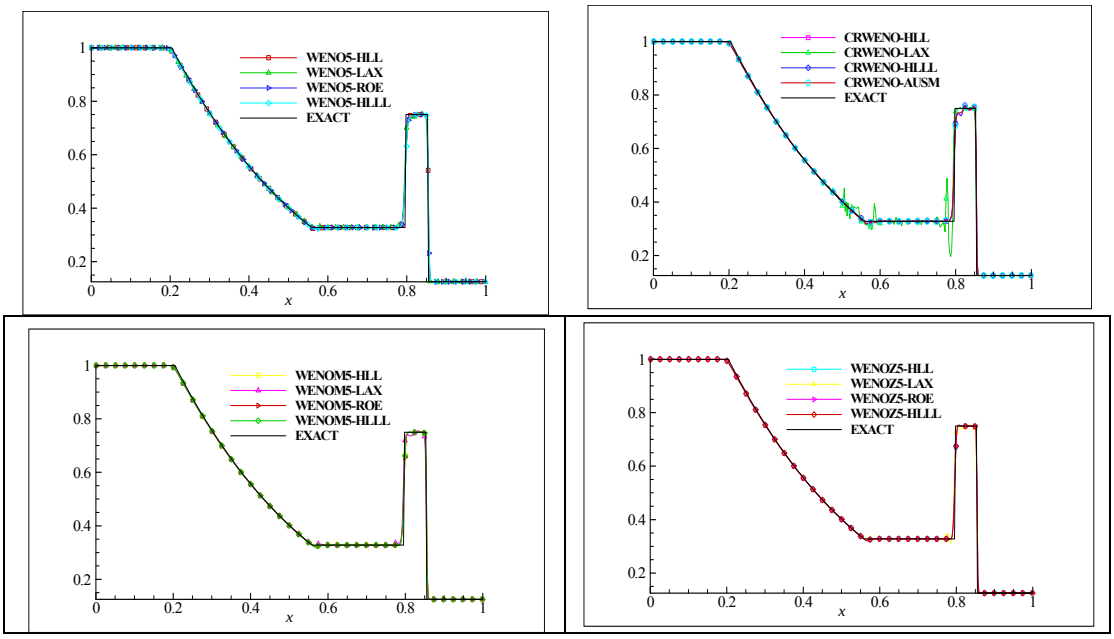

Fig. 3b. Numerical results for the density for the strong shock tube problem at t = 2.5 · 10^{-6}.

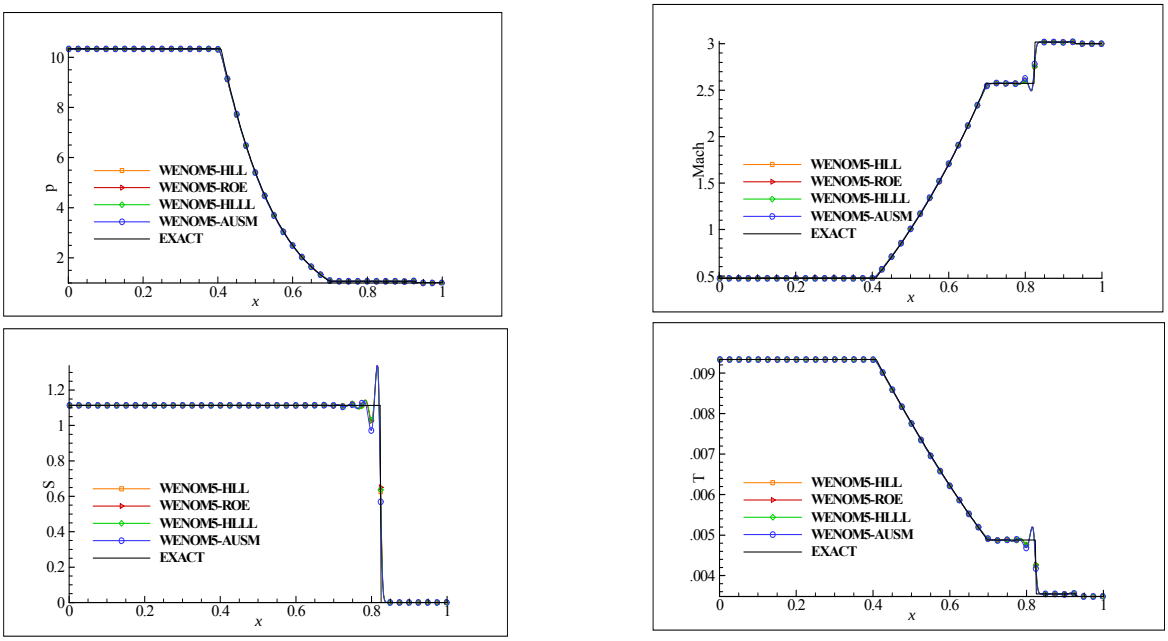

Fig. 4a. Pressure, Mach number, entropy and temperature evolution for of the Mach 3 shock tube problem at t = 0.09

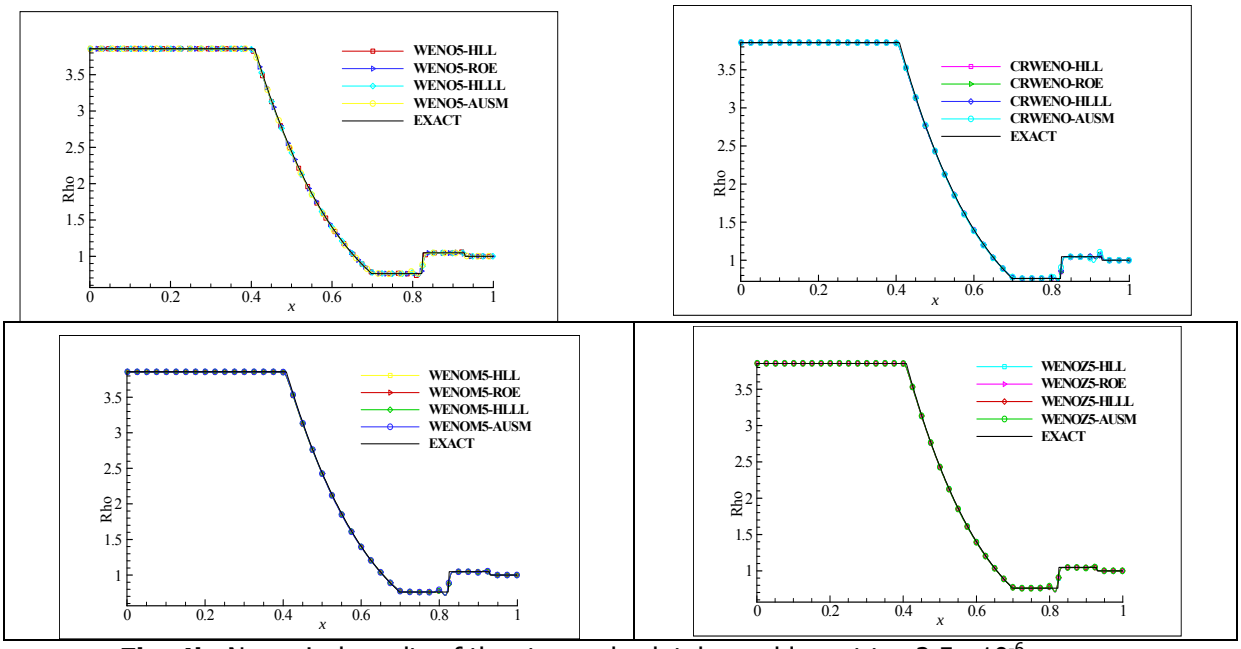

Fig. 4b. Numerical results of the strong shock tube problem at t = $2.5 \cdot 10^{-6}$.

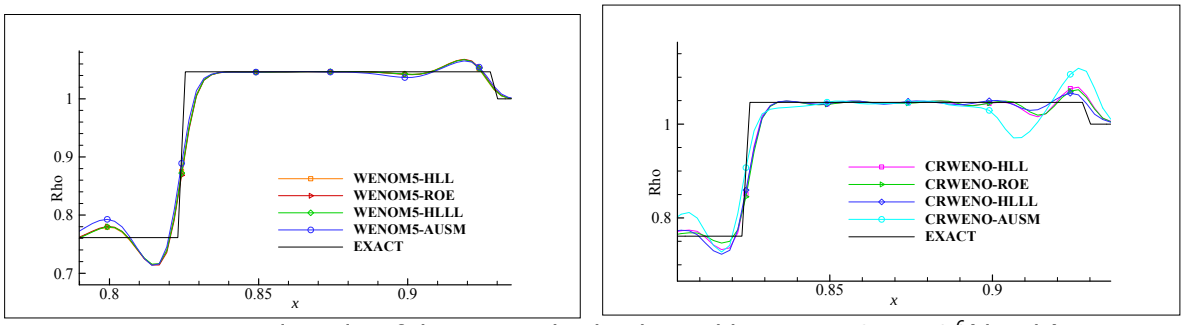

Fig. 4c. Numerical results of the strong shock tube problem at t = $2.5 \cdot 10^{-6}$(details).

d. Mach 3 shock test (expansion-contact-shock)

The Mach 3 shock tube experiment [17] uses the following initial conditions,

$$(\rho, u, p) = \begin{cases} (3.857, 0.92, 10.3333), & 0 \le x < 0.5 \\ (1, 3.55, 1), & 0.5 \le x \le 1 \end{cases} \tag{11}$$

and the final time is $t = 0.09$. Fig.4a shows no evident spurious oscillations at any shock or contact discontinuities except that the combination with Lax flux (not represented).In all cases we notice a small wavelet at shock discontinuity, see Fig. 4b and Fig. 4c.

e. High Mach flow test (shock-contact-shock)

The high Mach 3 shock tube experiment [19] uses the following initial conditions,

$$(\rho, u, p) = \begin{cases} (10, 2000, 500), & 0 \le x < 0.5 \\ (20, 0, 500), & 0.5 \le x \le 1 \end{cases} \tag{12}$$

and the final time is $t = 0.09$. Numerical solution using WENOM method is given in Fig. 5a. An unexpected result was discovered regarding CRWENO and WENO-Z method. We note that only WENO-JS and WENO-M gives numerical solutions to the problem.

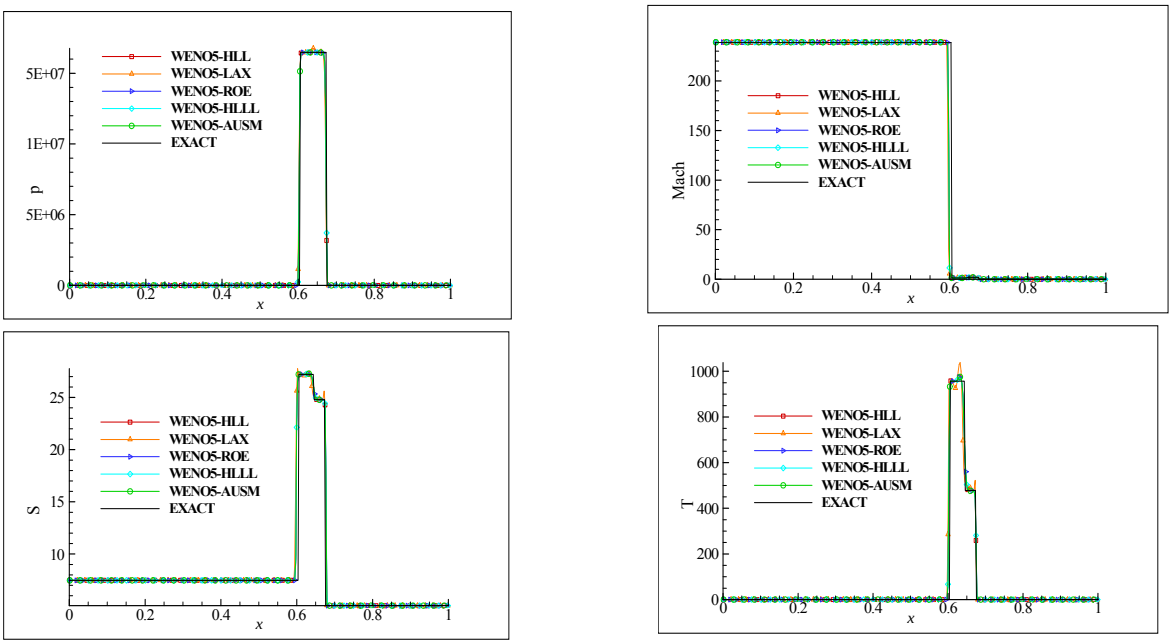

Fig. 5a. Pressure, Mach number, entropy and temperature evolution for high Mach number shock tube problem at t = $1.75 \cdot 10^{-4}$

3. Shock wave boundary layer interaction

3.1. The SUPERHYP code

The in-house code that has been developed (SUPERHYP) solves the time-dependent conservation law form of the RANS/LES equations. The spatial discretization involves a finite-volume approach. Upwind-biasing is used for the convective and pressure terms, while central differencing is used for the shear stress and heat transfer terms. Time advancement strategy allows solving steady or unsteady flows. This code is Fortran parallel code with a graphical interface to survey the solution during run. To account the air dissociation at high temperature fields the Park model and an interface with Chemkin code was also developed. For equilibrium flow the results of Gupta and all. [21] were adapted and implemented.

Code SUPERHYP solves the time-dependent conservation law form of the RANS/LES equations. The spatial discretization involves a semi-discrete finite-volume approach. Upwind-biasing is used for the convective and pressure terms, while central differencing is used for the shear stress and heat transfer terms. Time advancement strategy allows solving steady or unsteady flows. Grids must be supplied extraneously, but a mesh generator for simple geometries is included in the package.

SUPRHYP uses standard Fortran and will work on any machine with a compliant Fortran compiler (Fortran here denotes Fortran 90 or later - FORTRAN 77, FORTRAN 66, FORTRAN IV or other antiquated dialects are only supported to the extent that F90 is backward compatible). For distributed-memory parallelism, MPI can be used. In clustered architectures, OpenMP can be used for multiple processors on a node while MPI can be used between nodes.

3.2. Test cases

The laminar or turbulent flows over compression ramps with sharp leading edge is a typical shock-wave/boundary layer interaction problem (SWBLI). Fig. 6shows the system of shock waves present in supersonic/hypersonic flow around the ramp.

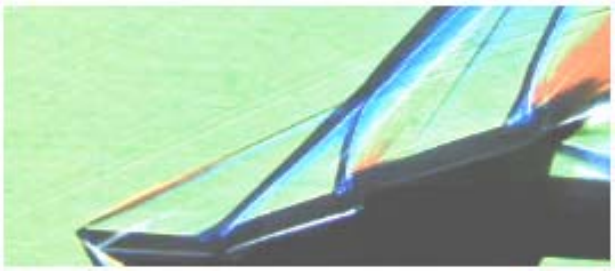

Fig.6 Schlieren photograph showing the flow configuration over the compression ramp in supersonic flow [22].

a) Test case 1.

The case corresponds to the experiments performed at the Calspan-UB Research Center wind tunnel [12] and reported by Marini [13]. The length of the flat plate is L = 0.4394 m and the ramp angle is 15 deg. To improve the boundary condition implementation in the leading edge of the horizontal plate, an upstream zone of 0.1 m length was added to the reference geometry. Flow conditions are: M_∞ = 11.63; Re_∞/m = 552116; T_∞ = 67.05 K and T_w = 294.38 K. Assuming the fluid air with constant thermodynamic proprieties the inflow velocity can be calculated, V_∞ = 1913.21 m/s.

The calculations were performed on a modest machine (INTEL I7 processor using 2 cores). The computational time was about 2 hours to reduce the residual (for axial velocity) up to 10^{-3}. The predicted results and the experimental results of Holden are presented in Fig.7 - Fig.9. In Fig.10 and Fig. 11 the calculated field variables Mach number and temperature are plotted.

b) Test case 2

This case was also investigated experimentally by Holden and Moselle [23]. The geometry is composed by a flat plate of length L = 0.4389 m, followed by a compression ramp of the same length, whose angle is θ = 24 deg. Flow conditions are: M_∞ = 14.1; Re_∞/m = 236200; T_∞ = 88.88 K and T_w = 297.22 K. An extended separation zone in vicinity of the ramp corner is present in this flow. Fig.12 plots the normalized pressure distribution along the wall. Obviously, the accuracy of the SUPERHYP code is very good. The pressure plateau in the separated region is very well predicted, Also the pressure distribution along the inclined wall is practically identical to the experimental data. However, the jump magnitude is slightly over predicted. The separation zone is also accurately calculated (Fig. 13). Not only the separation and the reattachment points are identified, but also the skin friction values in the separation zone correspond to the reference data. A good accuracy is obtained also for the Stanton number distribution (Fig.14). The shape of the distribution curve behind the corner is very well obtained, but the predicted position of the maximum value is slightly downstream with respect to the experimental data. Also, the maximum value is also somewhat under predicted. However, the differences are acceptable (maximum relative error is about 5%).

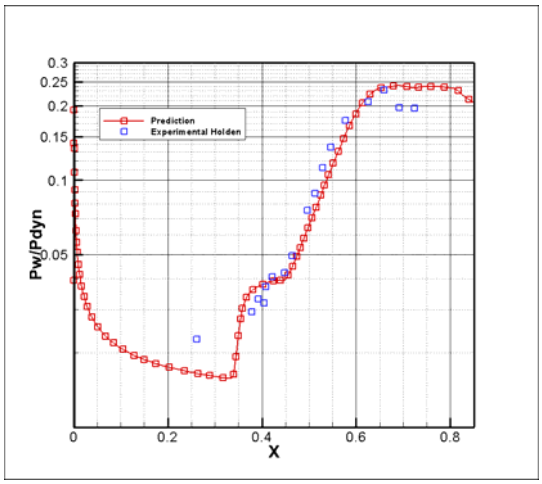

Fig. 7 Pressure distribution along the wall

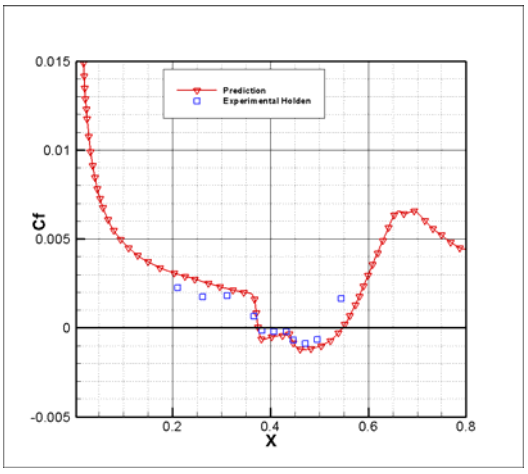

Fig. 8 Skin friction distribution along the wall

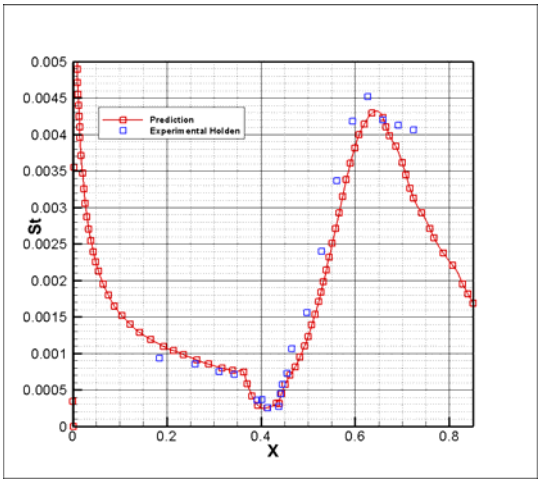

Fig. 9 Stanton number distribution along the wall

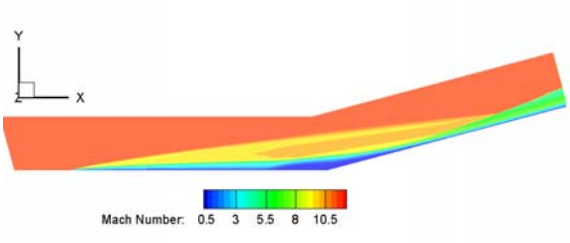

Fig.10 Mach number distribution

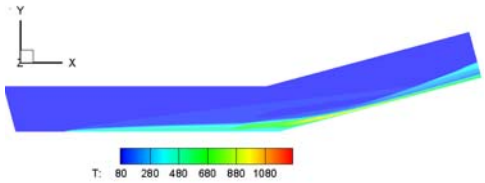

Fig. 11 Temperature field

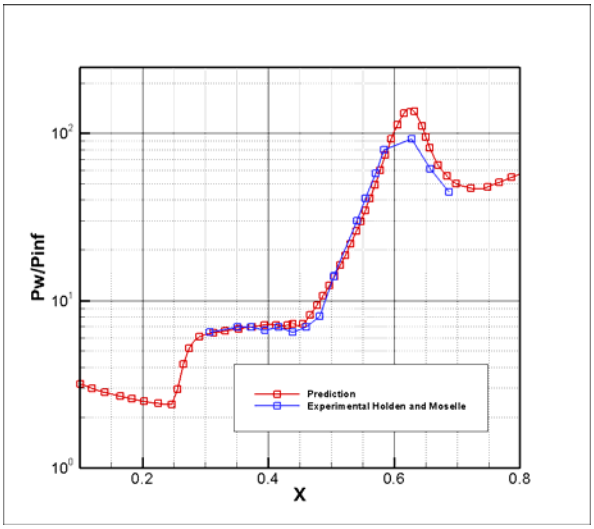

Fig.12 Normalized pressure distribution along the wall, case#2

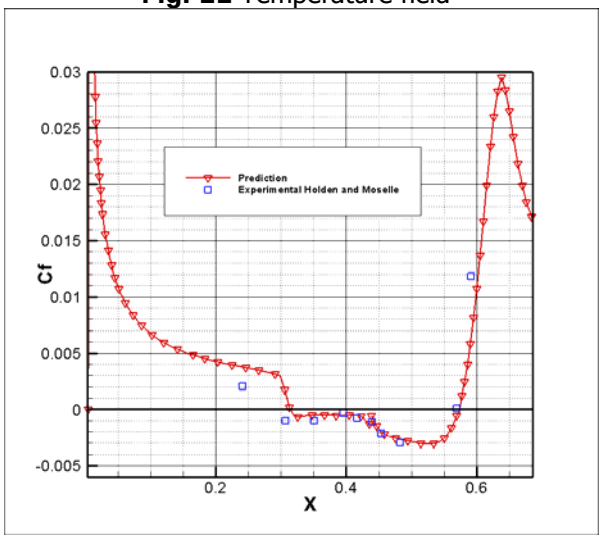

Fig.13. Skin friction distribution along the wall, case#2

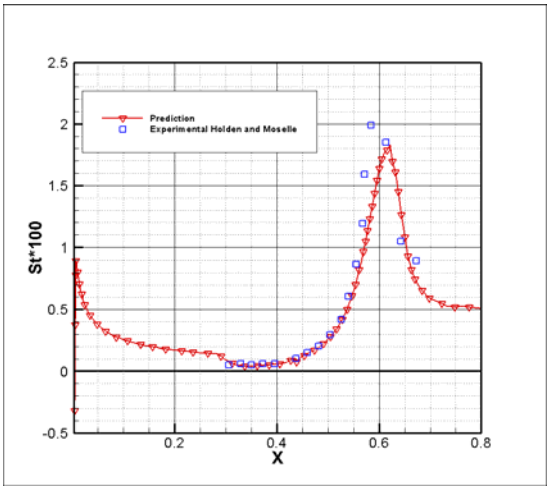

Fig.14 Stanton number distribution along the wall, case #2

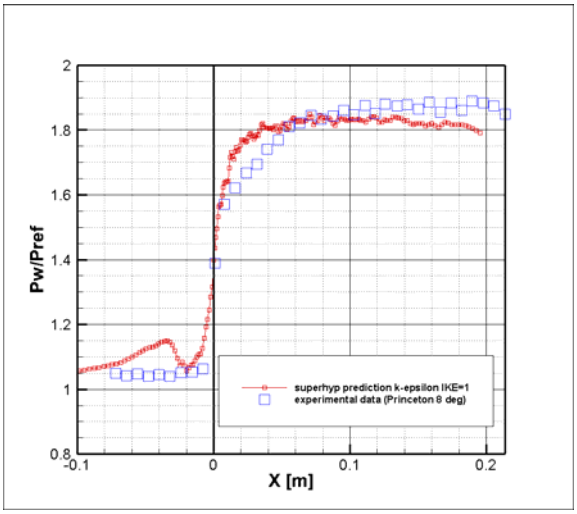

Fig. 15 Dimensionless pressure distribution along the wall for 8 deg Princeton compression ramp with k-epsilon turbulence model

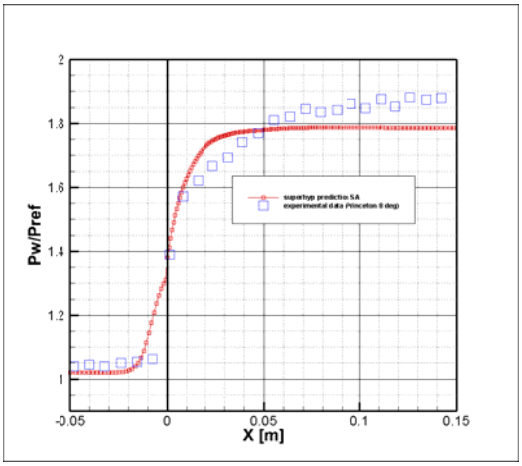

Fig. 16 Dimensionless pressure distribution along the wall for 8 deg Princeton compression ramp with Spalart-Almaras (SA) turbulence model.

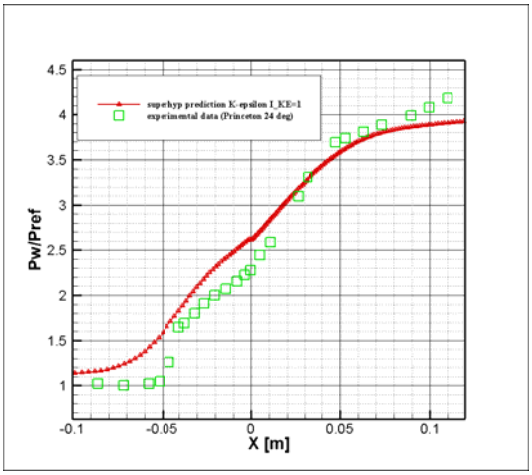

Fig.17 Pressure distribution for 24 deg Princeton compression ramp -k-epsilon model

On the ramp the pressure distribution oscillates, but similar behaviour is noticed inthe experimental data. For the Spalart-Almaras turbulence model, the results are like those given by the k-epsilon turbulence model. However, the asymptotic limit of pressure on the ramp is under predicted and the length of the detachment zone in front of the ramp is higher. Fig. 17 shows the pressure distribution on the 24 deg "Princeton ramp" [14].

4. Proper Orthogonal Decomposition

Proper Orthogonal Decomposition (POD) is a method [24] that reconstructs a data set from its projection onto an optimal base. Besides using an optimal base for reconstructing the data, the POD does not use any prior knowledge of the data set. Because the basis is only data dependent, POD is also used in analyzing the natural patterns of the flow field. The POD analysis for the above presented flows shows that the first two modes are monotone and reach a steady state. The higher modes become unsteady (oscillating) and cause the oscillation of the solution. Correlating with the shape of the higher modes we can identify the zones affected by oscillations. As expected, the higher modes present significant magnitudes atgrid points with sudden variation of parameters (along the shock wave). This behavior can be avoided "adapting" the mesh in the shock region and implementing non-oscillatory numerical schemes. However, the magnitudes of higher modes (starting with the third mode) near the wall are very small. Consequently, the wall distributions are not affected by oscillations and can be considered as a solution to the problem. Fig.18 shows the energy distribution on modes. The first 10 modes, containing 99.7% of the total energy, can be used for Reduced Order Model (ROM) reconstruction.

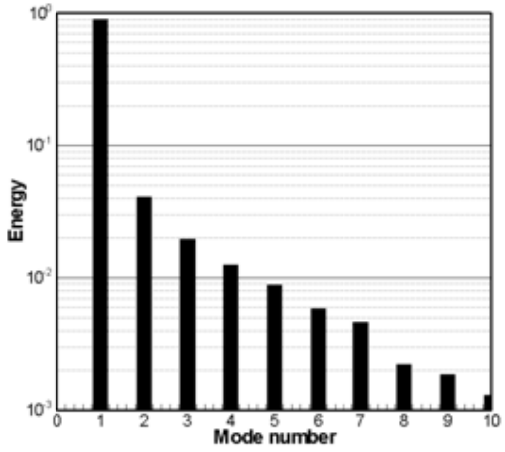

Fig. 18 Fraction of total energy for the most energetic modes

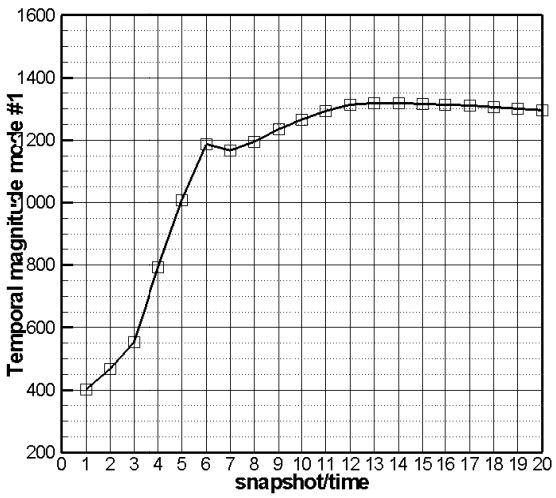

Fig.19 First mode amplitude variation.

Fig. 19 depict the temporal amplitude variation. The initial stages correspond to the formation of the shock waves as discussed above. Initial conditions assumed in the code setting influence the solution development on the first stages; for the last stages the main contribution in the solution belongs to the boundary conditions.

5. Conclusions

This paper is a continuation of the research from other papers [25, 26, 27] where we have analysed the behaviour and performances of different numerical schemes, in terms of accuracy and convergence properties. After the investigation of the advection equation and the scalar conservation equations with different initial conditions and different convex and non-convex conservative fluxes, we continued the research with the one-dimensional conservation equation. The code SUPERHYP was verified for a number of test experimental data available in literature. The cases correspond to the SWBL interaction problems at hypersonic velocities. For simple compression corner shock-boundary layer interactions, the results presented seem to indicate that, the RANS models are able of predicting surface pressures to a level of accuracy adequate for most engineering design work. However, much work remains before accurate predictions of the thermal environments over a flight vehicle may be obtained. The code predicts good results with respect to the reference data. We note the good stability of the numerical algorithm. The CFL number was considerably high during calculations (the adopted values were in the range from 1.5 to 2.5). To our best knowledge, similar codes in the available literature use CFL values around 0.05, especially for the first hundredsof iterations. The POD is used in analyzing the natural patterns of the flow field. The POD analysis shows that the first two modes are monotone and reach a steady state. The higher modes become unsteady (oscillating) and cause the oscillation of the solution. Correlating with the shape of the higher modes we can identify the zones affected by oscillations.

References

1. Shu, C.W: Essentially non-oscillatory and weighted essentially non-oscillatory schemes for hyperbolic conservation laws. NASA/CR-97-206253 ICASE Report. 97- 65 (1997)
2. Henrick A.K., Aslam T.D., Powers J.M.: Mapped weighted essentially non-oscillatory schemes: achieving optimal order near critical points. Journal of Computational Physics. 207, 542–567 (2005)
3. Ghosh D., Baeder J.D.: Compact Reconstruction Schemes with Weighted ENO Limiting for Hyperbolic Conservation Laws, SIAM Journal on Scientific Computing. 34, 1678–1706 (2012)
4. Acker F., Borges R. d. R., Costa B.: An improved weno-z scheme. Journal of Computational Physics. 313, 726–753 (2016)
5. Dănăilă S., Berbente C.: Metodenumericeîndinamicafluidelor (Numerical Methods in Fluid Dynamics). Ed. Academiei, Bucharest (2003)
6. Toro E.F.: Riemann Solvers and Numerical Methods for Fluid Dynamics: A Practical Introduction, third edition. Springer-Verlag (2009)
7. Linde T.: A Practical, Geeral-Purpose, Two-State HLL Riemann Solver for Hyperbolic Conservation Laws. International Journal for Numerical Methods Fluids. 40, 391-402 (2002)
8. Xiao F., Akoh R., Ii S.: Unified formulation for compressible and incompressible flows by using multi integrated moments II: multi-dimensional version for compressible and incompressible flows, Journal of Computational Physics. 213, 31-56 (2006)
9. Chapman D.R., Kuehn D.M., Larson H.K.: Investigation of Separated Flows in Supersonic and Subsonic Streams with Emphasis on the Effect of Transition. NACA-TN- 3869, NACA Rep. 1356, (1957)
10. Anderson J.D.: Hypersonic and High-Temperature Gas Dynamics, AIAA (2006).

11. Green J.E.: Interactions between shock waves and turbulent boundary layers. Prog. Aerosp. Sci. 11. 235–340 (1970)
12. Holden M.S.: Two-dimensional shock wave-boundary layer interactions in high speed flows. Part II, Experimental Studies on Shock Wave-Boundary Layer Interactions. AGARDograph AG-203 41–110 (1975)
13. Marini M.: Analysis of hypersonic compression ramp laminar flows under sharp leading edge conditions. Aerosp. Sci. Technol. 5, 257–271 (2001)
14. Settles G. S., Fitzpatrick T. J., Bogdonoff S. M.: Detailed Study of Attached and Separated Compression Corner Flow fields in High Reynolds Number Supersonic Flow. AIAA Journal. 17, 579–585 (1979)
15. Kuntz D., Amatucci V. A., Addy, A. L.: Turbulent Boundary-Layer Properties Downstream of the Shock-Wave/Boundary-Layer Interaction, AIAA Journal. 25, 668–675 (1987)
16. Aràndiga F., Baeza A., Belda A. M., Mulet P.: Analysis of WENO schemes for full and global accuracy. SIAM J. Numer. Anal. 49,893–915 (2011)
17. Harten A., Engquist B., Osher S., Chakravarthy S.R.: Uniformly high order accurate essentially non-oscillatory schemes, III. Journal of Computational Physics. 71, 231–303 (1987)
18. Liu X.-D., Osher S., Chan T.: Weighted essentially non-oscillatory schemes. Journal of Computational Physics. 115, 200–212, (1994)
19. Woodward P., Colella P.: The numerical simulation of two-dimensional fluid flow with strong shocks. Journal of Computational Physics. 54, 115 (1984)
20. Shu C. W., Osher S.: Efficient implementation of essentially nonoscillatory shock-capturing schemes, II. Journal of Computational Physics. 83, 32–78 (1989).
21. Gupta R.N., Lee K.P., Thomson R.A., Yos J.M..: Calculations and CurveFits of Thermodynamic andTransport Properties forEquilibrium Air to 30 000 K. NASA TR 1260, (1991).
22. Danaila S., Pricop M., Experimental results-Technical note, ESA-C- PR_WP5.4/TN-16, ESTEC Contract no. 4000109853/13/NL/SC, 2015
23. Holden M.S., Moselle J.R.: Theoretical and Experimental Studies for the Shock Wave-Boundary Layer Interaction on Compression Surfaces in Hypersonic Flow. ARL 70-0002. Aerospace Research Laboratories. Wright-Patterson AFB. Ohio, (1970)
24. Isvoranu D., Danaila S., Cizmas P., Leventiu C.: Proper Orthogonal Decomposition Applied to a Turbine Stage with In-Situ Combustion. In: Ahmet Yavuz Oral, Bahsi Oral, Banu Zehra (Eds.), 3rd International Congress on Energy Efficiency and Energy Related Materials (ENEFM2015) Proceedings, Springer Proceedings in Energy. 11-17 (2017
25. Bogoi A., Isvoranu D., Dănăilă S.: Assessment of some high-order finite difference schemes on the scalar conservation law with periodical conditions. INCAS BULLETIN. 8, 77–92 (2016)
26. Dănăilă S., Bogoi A., Isvoranu D.:Some Mandatory Benchmark Tests for Stability and Accuracy of High-Order Finite Difference Schemes. Applied Mechanics and Materials. 859, 52-56 (2017)
27. Bogoi A., Dănăilă S., Isvoranu D..: Assessment of three WENO type schemes for nonlinear conservative flux functions, INCAS BULLETIN, 10, 77 – 92 (2018)